Theor Chem Account (2008) 121:297–306
DOI 10.1007/s00214-008-0477-9

REGULAR ARTICLE

Quasirelativistic energy-consistent 5f-in-core pseudopotentials for pentavalent and hexavalent actinide elements

Anna Moritz · Michael Dolg

Received: 4 April 2008 / Accepted: 28 August 2008 / Published online: 18 September 2008

Abstract Quasirelativistic energy-consistent 5f-in-core pseudopotentials modeling pentavalent ($5f^{n-2}$ occupation with $n = 2$–6 for Pa–Am) and hexavalent ($5f^{n-3}$ occupation with $n = 3$–6 for U–Am) actinides have been adjusted. Energy-optimized (6s5p4d) and (7s6p5d) valence basis sets contracted to polarized double- to quadruple-zeta quality as well as 2f1g correlation functions have been derived. Corresponding smaller basis sets (4s4p3d) and (5s5p4d) suitable for calculations on actinide(V) and actinide(VI) ions in crystalline solids form subsets of these basis sets designed for calculations on neutral molecules. Calculations using the Hartree–Fock and the coupled-cluster method with single and double excitation operators and a perturbative estimate of triple excitations for actinide pentafluorides show satisfactory agreement with calculations using 5f-in-valence pseudopotentials and experimental data, respectively. However, in the hexavalent case the 5f-in-core approximation seems to reach its limitations except for hexavalent uranium ($5f^0$), where results for both uranium hexafluoride and the uranyl ion deviate only slightly from the 5f-in-valence reference data.

Keywords Actinides · Pseudopotentials · Valence basis sets · Actinide pentafluorides · Actinide hexafluorides · Uranyl ion

Electronic supplementary material The online version of this article (doi:10.1007/s00214-008-0477-9) contains supplementary material, which is available to authorized users.

A. Moritz (✉) · M. Dolg
Institut für Theoretische Chemie, Universität zu Köln,
Greinstr. 4, 50939 Cologne, Germany
e-mail: amoritz@uni-koeln.de; anna.moritz@uni-koeln.de

M. Dolg
e-mail: m.dolg@uni-koeln.de

1 Introduction

The chemical investigation of actinide elements and their compounds is important, particularly with regard to nuclear waste management, reprocessing nuclear fuel, and reduction of radiotoxicity. However, these studies involve several difficulties for both experimental and theoretical work. While the toxicity, radioactivity, and scarcity of the actinides are the main obstacles for the experimentalists [1], theoreticians face particular challenges in the significant contributions of relativity as well as electron correlation [2–5].

A commonly used approximation to cope with some of these problems in quantum chemical calculations is the pseudopotential (PP) approach, in which the explicit calculations are restricted to the chemically relevant valence electron system and relativistic effects are only implicitly accounted for by a proper adjustment of free parameters in the valence model Hamiltonian. For actinides two kinds of energy-consistent PPs with different core definitions, i.e. 5f-in-valence [6, 7] and 5f-in-core [8, 9] PPs, are available. The recently published 5f-in-core PPs avoid all difficulties due to the open 5f shell, and are therefore an efficient computational tool for those actinide compounds, where the 5f shell does not significantly contribute to bonding. Hence, calculations even on large molecules also containing several actinides become feasible. Furthermore, the 5f-in-core PPs might be a useful method for preoptimizing structures and getting an overview over low-lying electronic configurations prior to more rigorous studies on individual states including the 5f shell explicitly. Certainly, only electronic configurations with 5f occupations corresponding to that of the PP core can be considered, e.g. occupation changes between the 6d, 7s, or 7p shells are allowed.

Hartree–Fock (HF) test calculations on actinide di-, tri-, and tetrafluorides using 5f-in-core PPs show reasonable agreement with corresponding 5f-in-valence PP calculations except for PuF_2–CmF_2 and ThF_3/PaF_3, i.e. the m.a.e. (m.r.e.) in bond lengths and energies amount at most to 0.02 Å (0.9%) and 0.09 eV (2.5%) [8, 9]. The larger deviations for PuF_2–CmF_2 and ThF_3/PaF_3 are due to a configurational mixing of $5f^{n+1}$ with $5f^n6d^1$ and $5f^n$ with $5f^{n-1}6d^1$, respectively, whereby the assumption of a near-integral 5f occupation becomes too crude. A preliminary density functional theory (DFT) study on actinide(III) motexafin complexes (An–$Motex^{2+}$, An = Ac, Cm, Lr) demonstrates that the 5f-in-core approach performs encouragingly well [10]. A similar statement holds for the hydration behavior of trivalent actinide ions [11] and the investigation of actinocenes $An(C_8H_8)_2$ (An = Th–Pu) [12]. Furthermore, the trivalent 5f-in-core PP of uranium has successfully been used to calculate the cohesive energy of crystalline uranium nitride UN and its electron charge distribution [13]. Thus, despite the widespread common knowledge that the actinide 5f shell is chemically active and cannot be attributed to the core, we found ample quantitative evidence that such an approximation can be made without too much loss of accuracy for many cases. However, in the case of the higher, namely the penta- and hexavalent, oxidation states the successful applications will noticeably decrease compared to those of the lower (di-, tri-, and tetravalent) oxidation states, because the higher oxidation states are only formally realized in molecules.

Since the 5f orbitals are included in the core, one PP for each oxidation state, or rather, for each corresponding 5f subconfiguration is needed. Analogous to the recently published di-, tri-, and tetravalent 5f-in-core PPs, in this paper we present pentavalent ($5f^{n-2}$, $n = 2$–6 for Pa–Am) and hexavalent ($5f^{n-3}$, $n = 3$–6 for U–Am) 5f-in-core PPs together with various valence basis sets for use in calculations of molecules as well as solids. For these oxidation states no core-polarization potentials (CPPs) are provided, since the polarizability decreases with increasing charge of the PP core, and therefore the CPP effect would be even smaller than for the tetravalent PPs [9], where the bond lengths and energies of AnF_4 changed only by about 0.007 Å and 0.005 eV, respectively, if CPPs are used. Results of HF test calculations using the newly developed penta- and hexavalent PPs for actinide pentafluorides AnF_5 (An = Pa–Am) and hexafluorides AnF_6 (An = U–Am) are compared to corresponding calculations using 5f-in-valence PPs. In cases where experimental or all-electron (AE) data are available, also coupled-cluster calculations with single and double excitation operators and a perturbative estimate of triple excitations [CCSD(T)] are discussed. Furthermore, the uranyl ion UO_2^{2+} is investigated at the HF, CCSD(T), and DFT level using both the 5f-in-core and 5f-in-valence PP.

2 Method

The method of relativistic energy-consistent ab initio pseudopotentials is described in detail elsewhere [6, 14, 15] and will be outlined here only briefly. The valence-only model Hamiltonian for a system with n valence electrons and N nuclei with charges Q is given as

$$H_v = -\frac{1}{2}\sum_i^n \Delta_i + \sum_{i<j}^n \frac{1}{r_{ij}} + \sum_i^n \sum_I^N V_I(r_i) + \sum_{I<J}^N \frac{Q_I Q_J}{R_{IJ}}. \tag{1}$$

Here i and j are electron indices, I and J are nuclear indices. $V_I(r_i)$ denotes a semilocal effective core potential (ECP) for nucleus I

$$V_I(r_i) = -\frac{Q_I}{r_{Ii}} + \sum_l \sum_k A^I_{lk} \exp\left(-a^I_{lk} r^2_{Ii}\right) P^I_l. \tag{2}$$

P^I_l is the projection operator onto the Hilbert subspace of nucleus I with angular momentum l

$$P^I_l = \sum_{m_l} |lm_l\rangle\langle lm_l|. \tag{3}$$

The 5f-in-core PPs corresponding to pentavalent ($5f^{n-2}$, $n = 2$–6 for Pa–Am) and hexavalent ($5f^{n-3}$, $n = 3$–6 for U–Am) actinide atoms were generated analogous to the trivalent ($5f^n$, $n = 0$–14 for Ac–Lr) [8] and to the divalent ($5f^{n+1}$, $n = 5$–13 for Pu–No) as well as tetravalent ($5f^{n-1}$, $n = 1$–9 for Th–Cf) [9] PPs. The 1s–5f (spherically averaged) shells are included in the PP core, while all orbitals with main quantum number larger than five are treated explicitly, i.e. 13 and 14 valence electrons for the penta- and hexavalent PPs, respectively. The s-PPs are composed of three and the p- and d-PPs of two Gaussians, which were adjusted by a least-squares fit to the total valence energies of 18 reference states (pentavalent PPs: An $6d^37s^2$, $6d^47s^1$, $6d^5$, $6d^27s^27p^1$, $6d^37s^17p^1$, An^+ $6d^37s^1$, $6d^27s^2$, $6d^4$, $6d^27s^17p^1$, $6d^37p^1$, An^{2+} $6d^3$, $6d^27s^1$, $6d^17s^2$, $6d^27p^1$, $6d^17s^17p^1$, An^{3+} $6d^2$, $6d^17s^1$, $7s^2$; hexavalent PPs: An $6d^47s^2$, $6d^47s^17p^1$, $6d^37s^27p^1$, $6d^27s^27p^2$, An^+ $6d^47s^1$, $6d^5$, $6d^37s^2$, $6d^47p^1$, $6d^37s^17p^1$, An^{2+} $6d^4$, $6d^37s^1$, $6d^27s^2$, $6d^37p^1$, $6d^27s^17p^1$, An^{3+} $6d^3$, $6d^27s^1$, $6d^17s^2$, $6d^27p^1$). The reference data were taken from relativistic AE calculations using the so-called Wood–Boring (WB) scalar-relativistic HF approach. A brief description of the computational details was given in previous publications [14, 16]. Both AE WB as well as PP calculations were performed with an atomic finite-difference HF scheme [17]. In order to allow for some participation of the 5f orbitals in chemical bonding the f-parts of the PPs are designed to describe partial occupations of the 5f shell, which are larger than the integral occupation number implied by the valency, i.e. $5f^{n-2+q}$ ($n = 2$–6 for Pa–Am) and $5f^{n-3+q}$ ($n = 3$–6 for

U–Am) with $0 \leq q < 1$ for penta- and hexavalent actinide atoms, respectively [18]. These f-PPs consist of two types of potentials V_1 and V_2 which are linearly combined as follows [8]

$$V = \left(1 - \frac{m}{14}\right)V_1 + \frac{m}{14}V_2. \quad (4)$$

Here m is the integral number of electrons in the 5f orbitals kept in the core, i.e. $m = n-2$ and $m = n-3$ for the penta- and hexavalent case, respectively. V_1 and V_2 model 5f shells, which can and respectively cannot accommodate an additional electron. Thus, V_1 is the exact potential for a $5f^0$ occupation, whereas V_2 is exact for $5f^{14}$. For pentavalent PPs the errors in the total valence energies of finite-difference HF calculations are smaller than 0.06 and 0.30 eV for s-, p-, d- and f-parts, respectively. For hexavalent PPs these errors are smaller than 0.03 and 0.76 eV. Since the errors for f-PPs are quite large, we tried to use two Gaussians for V_1 and V_2. In this way the deviations could be clearly reduced to at most 0.05 eV for both penta- and hexavalent PPs. However, these f-PPs yield too strong 5f orbital participations especially in the case of $5f^0$, i.e. for Pa(V) and U(VI) large-core PP (LPP) 5f occupations are by 0.15 and 0.52 electrons larger than small-core PP (SPP) 5f occupations, respectively (5f occupations for LPP/SPP: Pa(V) 0.71/0.56; U(VI) 1.68/1.16). Moreover, the deviations between LPP and SPP bond lengths and energies are at least twice as large, if two Gaussians instead of one are used for V_1 and V_2 (f-PP with one/two Gaussians: Pa(V) $\Delta R_{ax} = 0.013/0.032$ Å, $\Delta R_{eq} = 0.012/0.039$ Å, $\Delta E = 0.052/0.334$ eV; U(VI) $\Delta R = 0.0004/0.042$ Å, $\Delta E = 0.29/0.68$ eV). Thus, we use only one Gaussian for V_1 and V_2 and accept the greater errors of 0.30 (0.4%) and 0.76 eV (0.7%) for the total valence energies of Pa^{12+} and U^{13+} for the adjustment of penta- and hexavalent f-PPs, respectively, to avoid a too strong 5f orbital participation.

The Gaussian type orbital (GTO) valence basis sets were constructed analogous to those for di- and tetravalent PPs [9]. First, basis sets for use in crystal calculations were created, i.e. (4s4p3d) and (5s5p4d) basis sets were HF energy-optimized [19] for the valence subconfiguration $6s^2 6p^6 6d^1$ of fourfold- and fivefold-charged actinide cations in the case of penta- and hexavalent PPs, respectively. All exponents that became smaller than 0.15 were fixed to this value and the remaining exponents were reoptimized. Furthermore, all optimizations were carried out with the requirement that the ratio of exponents in the same angular symmetry must be at least 1.5. The basis set errors in the valence energies with respect to numerical finite-difference LPP HF calculations are below 0.09 and 0.02 eV for (4s4p3d) and (5s5p4d) of pentavalent PPs, respectively. For hexavalent PPs these errors are smaller than 0.13 and 0.03 eV.

Secondly, the valence basis sets were augmented by adding a set of 2s1p1d low-exponent Gaussians yielding (6s5p4d) and (7s6p5d) primitive sets for use in molecular calculations. The added exponents were HF energy-optimized [19] for the $6d^3 7s^2$ and the $6d^4 7s^2$ valence subconfiguration of the neutral actinides for penta- and hexavalent PPs, respectively. For pentavalent PPs the differences in the valence energies with respect to numerical finite-difference LPP HF calculations are at most 0.10 and 0.02 eV for (6s5p4d) and (7s6p5d), respectively. For hexavalent PPs these errors are at most 0.15 and 0.05 eV.

Thirdly, the basis sets were contracted using different segmented contraction schemes to yield basis sets of approximately valence double-, triple-, and quadruple-zeta quality (VDZ, VTZ, and VQZ) for the s and p symmetries. In the case of d symmetry at least a triple-zeta contraction was necessary and additional sets with a less tight d contraction are also offered (VDZ: [4s3p3d], VTZ: [5s4p3d], [5s4p4d], and VQZ: [6s5p4d]). For pentavalent PPs the errors in total valence energies of the $6d^3 7s^2$ valence substates with respect to numerical finite-difference LPP HF calculations for the contracted (6s5p4d) basis sets, the VDZ as well as the VTZ contracted (7s6p5d) basis sets, and the VQZ contracted (7s6p5d) basis sets are below 0.17, 0.08, and 0.03 eV, respectively. For hexavalent PPs these errors in total valence energies of the $6d^4 7s^2$ valence substates are smaller than 0.33, 0.13, and 0.06 eV, respectively.

Fourthly, sets of 2f1g polarization functions were energy-optimized in configuration interaction (CI) calculations [20] for the $6d^3 7s^2$ and $6d^4 7s^2$ valence subconfiguration of penta- and hexavalent PPs, respectively. The parameters of PPs and basis sets are compiled in the electronic supplementary material of this publication. They are also available from the authors and will be incorporated, e.g. into the MOLPRO [20] basis set library [21].

The test calculations for AnF_5 (An = Pa–Am) and AnF_6 (An = U–Am) were carried out with the MOLPRO program package [20] using penta- and hexavalent 5f-in-core LPPs (large-core PP with 13 and 14 valence electrons and 78–82 (Pa–Am) and 78–81 (U–Am) core electrons, respectively) as well as 5f-in-valence SPPs [6] (small-core PP with 60 core electrons and 31–35 (Pa–Am) valence electrons). For F Dunning's aug-cc-pVQZ (augmented correlation-consistent polarized VQZ) basis set [22, 23] was applied and for An (7s6p5d2f1g)/[6s5p4d2f1g] and (14s13p10d8f6g)/[6s6p5d4f3g] [7] valence basis sets were used for LPP HF and SPP state-averaged multiconfiguration self-consistent field (MCSCF) calculations, respectively. The state-averaging was necessary to avoid symmetry-breaking at the orbital level, since the program MOLPRO is limited to the D_{2h} point group and subgroups. The AnF_5 and AnF_6 geometries were optimized implying

C_{4v} and O_h symmetry, respectively. For PaF_5 and UF_5 as well as for UF_6, NpF_6, and PuF_6 also LPP CCSD(T) calculations were performed, since for these compounds experimental or AE results are available [24–27]. In the CCSD(T) calculations the F 1s orbitals were chosen to be frozen.

For UO_2^{2+}, HF and CCSD(T) calculations were carried out with MOLPRO implying $D_{\infty h}$ symmetry using both the 5f-in-core and 5f-in-valence PP. For O Dunning's aug-cc-pVQZ basis set [22, 23] was applied and for An (7s6p5d2f1g)/[6s5p4d2f1g] and (14s13p10d8f6g)/[6s6p5d4f3g] [7] valence basis sets were used for LPP and SPP, respectively. In the CCSD(T) calculations the O 1s orbitals were kept frozen. Furthermore, a LPP and SPP DFT/B3LYP [28–33] calculation were performed with TURBOMOLE v. 5.7 [34] applying D_{6h} symmetry. Since in TURBOMOLE v. 5.7 exchange–correlation energies are numerically integrated on element specific grids, and since no grid for uranium is implemented, the LPP and SPP calculations were carried out employing the cerium and tungsten m5 grid, respectively, by calculating the corresponding CeO_2^{2+} and WO_2^{2+} molecules and by setting the Ce and W nuclear charge and mass to 92 and 238.03 u, respectively. In the case of the SPP DFT calculations segmented contracted (14s13p10d8f6g)/[10s9p5d4f3g] [35] valence basis sets were used.

3 Results and discussion

The results for some properties (namely bond length, bond angle, and binding energy) of AnF_5 (An = Pa–Am), AnF_6 (An = U–Am), and UO_2^{2+} will be presented here to demonstrate the transferability of the 5f-in-core PPs and the corresponding basis sets to a molecular environment.

The An–F bond energy was calculated by $E_{\text{bond}} = [E(\text{An}) + n \times E(F) - E(\text{AnF}_n)]/n$ (with $n = 5, 6$ for AnF_5, AnF_6), where the actinide atom was assumed to be in the lowest valence substate, i.e. $5f^{n-2}6d^37s^2$ and $5f^{n-3}6d^47s^2$ for AnF_5 and AnF_6, respectively. At this point one might ask how to calculate a binding energy with respect to the experimentally observed ground states of the actinides. We suggest to follow the strategy proposed for the lanthanide PPs almost two decades ago [36]. First, one should calculate the binding energy with respect to the actinide atom in its lowest valence substate corresponding to the $5f^{n-2}$ and $5f^{n-3}$ subconfiguration for penta- and hexavalent LPPs, respectively. Then the energy difference to the experimentally observed ground state can be determined, e.g. at the AE WB [17] or Dirac–Hartree–Fock [37] level, and this difference has to be subtracted from the binding energy calculated with respect to the lowest valence substate corresponding to $5f^{n-2}$ and $5f^{n-3}$, respectively. In contrast to di-, tri-, and tetravalent PPs for penta- and hexavalent PPs an energy correction using experimental energy differences is not possible, since for the $6d^37s^2$ and the $6d^47s^2$ valence subconfiguration no experimental data are available [38]. If desired, correlation contributions can be obtained by 5f-in-valence PP or AE atomic calculations. Tables summarizing some possible corrections are included in the electronic supplementary material.

The ionic binding energy of UO_2^{2+} was defined by $\Delta E = E(U^{6+}) + 2 \times E(O^{2-}) - E(UO_2^{2+})$.

3.1 Actinide pentafluorides

The LPP HF and CCSD(T) calculations for AnF_5 (An = Pa–Am) will be compared to corresponding SPP state-averaged MCSCF calculations as well as to experimental [25] and computational [24, 39, 40] data from the literature. The results for bond lengths, angles, as well as energies and those of a Mulliken population analysis are listed in Tables 1 and 2, respectively.

3.1.1 Molecular structure

While in 1977 the infrared spectrum of UF_5 [25] indicated a C_{4v} symmetry, later computational studies [39] including relativistic effects (also spin–orbit coupling) showed the D_{3h} geometry to be 1 kcal mol^{-1} lower than the C_{4v} one. This finding is not contradictory to the experimental result, since in the photogeneration of UF_5 from UF_6 one has an internal energy excess of more than 1 kcal mol^{-1}. We decided to perform the geometry optimizations imposing

Table 1 An–F bond lengths R_{ax} and R_{eq} (in Å) and angles $\angle F_{\text{ax}}$ – An–F_{eq} (in deg) as well as bond energies E_{bond} (in eV) for AnF_5 (An = Pa–Am) from LPP HF and SPP state-averaged MCSCF calculations

An	R_{ax}		R_{eq}		$\angle$		E_{bond}	
	LPP	SPP[a]	LPP	SPP[a]	LPP	SPP[a]	LPP	SPP
Pa	2.034	2.047	2.027	2.040	106.8	105.6	5.556	5.504
	2.035	*2.061*	*2.023*	*2.060*	*106.4*	*100.3*	*7.086*	
U	2.028	2.026	2.028	2.022	107.5	105.7	5.263	5.386
	2.032	*2.00*	*2.028*	*2.02*	*107.4*	*101*	*6.759*	
Np	2.017	2.008	2.021	2.007	107.7	103.9	5.099	5.255
Pu	2.002	1.996	2.009	1.996	107.7	104.7	5.003	5.092
Am	1.988	1.982	1.998	1.987	107.6	104.5	4.933	4.962

For PaF_5 and UF_5 LPP CCSD(T) and AE DFT [24] as well as experimental [25] data are given in italics

Basis sets: LPP (7s6p5d2f1g)/[6s5p4d2f1g]; SPP (14s13p10d8f6g)/[6s6p5d4f3g]; F aug-cc-pVQZ

[a] Given in italics: PaF_5: AE DFT/BP86 results using ZORA and pVTZ basis sets; UF_5: experimental values

Table 2 Mulliken 6s/7s, 6p, 6d, and 5f orbital populations and atomic charges (Q) on An in AnF$_5$ (An = Pa–Am) from LPP HF and SPP state-averaged MCSCF calculations

An	s		p		d		f		Q	
	LPP	SPP	LPP	SPP	LPP	SPP	LPP[a]	SPP	LPP	SPP
Pa	1.96	2.19	5.84	5.85	0.66	0.85	0.56	0.56	3.96	3.53
U	1.96	2.20	5.83	5.80	0.72	0.86	0.42	1.55	4.05	3.58
Np	1.96	2.22	5.82	5.79	0.76	0.92	0.36	2.60	4.07	3.46
Pu	1.96	2.24	5.82	5.80	0.80	0.98	0.33	3.61	4.07	3.36
Am	1.96	2.26	5.81	5.82	0.83	1.05	0.31	4.63	4.07	3.24

A $6s^2 6p^6 6d^3 7s^2$ ground state valence subconfiguration is considered for An. Basis sets: LPP (7s6p5d2f1g)/[6s5p4d2f1g]; SPP (14s13p10d8f6g)/[6s6p5d4f3g]; F aug-cc-pVQZ

[a] Zero to four electrons in the 5f shell are attributed to the LPP core for Pa–Am, respectively

C_{4v} symmetry, so that the LPP results can also be compared to experimental values.

Due to the actinide contraction the An–F bond lengths calculated by using LPP HF and SPP state-averaged MCSCF decrease continuously with increasing nuclear charge. The decrease of axial bond lengths R_{ax} is slightly larger than that of equatorial bond lengths R_{eq}, since the axial ligand experiences a lower ligand–ligand repulsion than the equatorial ligands (LPP: $\Delta R_{\mathrm{ax}} = 0.05$ Å, $\Delta R_{\mathrm{eq}} = 0.03$ Å; SPP: $\Delta R_{\mathrm{ax}} = 0.07$ Å, $\Delta R_{\mathrm{eq}} = 0.05$ Å). The F_{ax}–An–F_{eq} bond angles $\angle$ stay almost constant along the actinide row, i.e. the deviation between angles of different actinides amount at most to 0.9 and 1.8° for LPPs and SPPs, respectively.

The An–F bond lengths R_{ax} and R_{eq} from LPP HF calculations are in good agreement with the SPP reference data, i.e. the mean absolute error (m.a.e.) and the mean relative error (m.r.e.) amount to 0.007 (0.4%) and 0.011 Å (0.5%) for R_{ax} and R_{eq}, respectively. The maximum error for both bond lengths is 0.013 Å (0.7%). The deviations between LPP and SPP bond angles are slightly larger, i.e. the m.a.e. (m.r.e.) and the maximum error amount to 2.6 (2.5%) and 3.8° (3.7%), respectively. Furthermore, the LPP HF structure for UF$_5$ is comparable to that of a former HF calculation, where a Cowan–Griffin ECP for U and VDZ basis sets were used (ECP HF for UF$_5$: $R_{\mathrm{ax}} = 2.00$ Å, $R_{\mathrm{eq}} = 2.00$ Å, $\angle = 100°$) [39]. The deviations in bond lengths and angles are 0.03 Å (1.4%) and 8° (8.0%), respectively.

If correlation is included via CCSD(T), the molecular structures of PaF$_5$ and UF$_5$ change only slightly by at most 0.004 Å and 0.4°. For PaF$_5$ the deviations between LPP CCSD(T) results and AE DFT/BP86 calculations using the zero-order regular approximation (ZORA) and pVTZ basis sets [24] amount to 0.026, 0.037 Å, and 6.1° for R_{ax}, R_{eq}, and $\angle$, respectively. For UF$_5$ the differences between LPP CCSD(T) and experimental [25] results are 0.03, 0.01 Å, and 6° for R_{ax}, R_{eq}, and $\angle$, respectively. Moreover, the comparison to the UF$_5$ structure calculated by SPP DFT/PBE0 using pVDZ basis sets [40] gives deviations of just 0.018, 0.013 Å, and 9.1° for R_{ax}, R_{eq}, and $\angle$, respectively (SPP DFT/PBE0 for UF$_5$: $R_{\mathrm{ax}} = 2.014$ Å, $R_{\mathrm{eq}} = 2.015$ Å, $\angle = 98.3°$). Thus, the LPP CCSD(T) results are also in good agreement with corresponding reference data and confirm the reliability of the newly developed LPPs.

3.1.2 Bond energy

The An–F bond energy of AnF$_5$ decreases by 0.62 and 0.54 eV with increasing nuclear charge for LPP HF and SPP state-averaged MCSCF calculations, respectively. This is related to the increasing F–F repulsion, which is due to the decreasing An–F bond length.

The LPP and SPP An–F bond energies are in good agreement, i.e. the m.a.e. (m.r.e.) amounts to 0.090 eV (1.7%) and the maximum error, which occurs for neptunium, is 0.16 eV (3.0%). As expected the inclusion of electron correlation via CCSD(T) clearly increases the An–F bond energies by ca. 1.5 eV.

3.1.3 Mulliken orbital populations

The Mulliken orbital populations show that the bonding in AnF$_5$ is basically ionic with significant back-bonding into the An 6d and 5f (less 7s) orbitals. For LPP and SPP calculations this results in charge separations up to 0.81 and 0.72 electrons per bond and in total atomic charges of up to 4.07 and 3.58 units on the actinide, respectively. The SPP 5f occupations vary on average by 0.59 electrons and at most by 0.63 electrons from the assumed LPP $5f^{n-2}$ occupations, which demonstrates that the 5f orbitals participate to some extent in the An–F bonding. However, the 5f-in-core approach still yields reasonable results, since the differences between LPP and SPP 5f occupations amount on average only to 0.19 electrons and at most to 0.32 electrons, because the f-part of the LPPs allows for some 5f occupation in addition to the integral $5f^{n-2}$ assumption.

3.2 Actinide hexafluorides

The LPP HF and CCSD(T) calculations for AnF$_6$ (An = U–Am) will be compared to SPP state-averaged MCSCF results and experimental [26, 27] as well as computational [41–43] data from literature. The Mulliken orbital population analysis will not be discussed in detail, because it leads to similar conclusions as for AnF$_5$. However, the 5f orbital populations will be given together with the other results as well as the available experimental data in Table 3.

Table 3 An–F bond lengths R (in Å), bond energies E_{bond} (in eV), and 5f orbital occupations for AnF_6 (An = U–Am) from LPP HF and SPP state-averaged MCSCF calculations

An	R				E_{bond}			5f Occupation	
	LPP HF	SPP	LPP CC	Exp.[a]	LPP HF	SPP	LPP CC	LPP[b]	SPP
U	1.976	1.975	1.978	1.996(8)	5.355	5.646	6.931	0.96	1.16
Np	1.983	1.966	1.988	1.981(8)	4.813	5.499	6.360	0.67	2.28
Pu	1.980	1.949	1.989	1.971(10)	4.542	5.439	6.093	0.56	3.46
Am	1.965	1.941			4.479	5.279		0.59	4.52

For UF_6, NpF_6, and PuF_6 LPP CCSD(T) and experimental [26] results are given, too

Basis sets: LPP (7s6p5d2f1g)/[6s5p4d2f1g]; SPP (14s13p10d8f6g)/[6s6p5d4f3g]; F aug-cc-pVQZ

[a] For UF_6 also another experimental value is available: $R = 1.999$ (3) Å [27]

[b] Zero to three electrons in the 5f shell are attributed to the LPP core for U–Am, respectively

3.2.1 Molecular structure

The An–F bond lengths calculated by using LPPs at the HF level increase from UF_6 to NpF_6 by 0.007 Å and decrease from NpF_6 to AmF_6 by 0.018 Å. The SPP state-averaged MCSCF bond lengths, however, decrease smoothly with increasing nuclear charge by 0.034 Å. While the reason for the decrease is the well-known actinide contraction, the increase from UF_6 to NpF_6 is possibly due to a shortcoming of the LPP method, because for the equatorial bond length of AnF_5 an analogous, but clearly smaller, increase from PaF_5 to UF_5 by 0.001 Å is obtained (cf. Table 1). Since the U–F bond length is only by ca. 0.02 Å smaller than expected, this LPP shortcoming is still acceptable.

The LPP HF results are in good agreement with the SPP reference data, i.e. the LPP An–F distances are at most by 0.031 Å (1.6%) too long and the m.a.e. (m.r.e.) amount to 0.018 Å (0.9%). For UF_6, NpF_6, and PuF_6 the comparison of our LPP HF bond lengths to those of HF calculations [41], where Cowan–Griffin ECPs for An and pVDZ basis sets were used, shows also satisfactory results, i.e. the maximum error amounts to 0.037 Å (1.9%) (ECP HF: UF_6 $R = 1.984$, NpF_6 $R = 1.972$, PuF_6 $R = 1.943$ Å). Moreover, the obtained U–F bond length is also in good agreement with that determined by a SPP HF calculation [43] using an aug-pVDZ basis set for F, i.e. the bond lengths deviate by 0.009 Å (0.5%) (SPP HF: UF_6 $R = 1.985$ Å). Thus, in the case of the An–F bond lengths the hexavalent 5f-in-core approximation still holds, although the calculated SPP 5f occupations are about 1.35 electrons larger than the integral LPP occupations and even the differences between the LPP and SPP 5f occupations amount to ca. 0.66 electrons.

Analogous to the AnF_5 results the introduction of correlation via CCSD(T) increases the An–F bond lengths only slightly by at most 0.009 Å. The differences between LPP CCSD(T) and experimental [26] data are at most 0.018 Å (0.9%) and the m.a.e. (m.r.e.) amounts to 0.014 Å (0.7%). Compared to DFT data from literature [41–43] the LPP CCSD(T) bond lengths deviate at most by 0.036 Å (1.8%) (ECP DFT/B3LYP [41]: UF_6 $R = 2.014$, NpF_6 $R = 2.013$, PuF_6 $R = 1.985$ Å; SPP DFT/B3LYP [42]: UF_6 $R = 2.007$, NpF_6 $R = 1.991$, PuF_6 $R = 1.977$ Å; SPP DFT/PBE0 [43]: UF_6 $R = 1.993$ Å). Therefore, the correlated calculations of AnF_6 (An = U–Pu) confirm the good performance of the hexavalent 5f-in-core PPs for the An–F bond lengths.

3.2.2 Bond energy

The An–F bond energies decrease continuously with increasing nuclear charge by 0.88 and 0.37 eV for LPP and SPP calculations, respectively. This is due to the increasing F–F repulsion with decreasing An–F distances as it is the case for AnF_5.

In contrast to the good agreement for the An–F bond lengths, the LPP HF bond energies of AnF_6 deviate considerably from the SPP state-averaged MCSCF data, i.e. the m.a.e. (m.r.e.) and the maximum difference are 0.67 (12.3%) and 0.80 eV (15.2%), respectively. These significant discrepancies are in line with the high differences between LPP and SPP 5f orbital occupations of up to 0.93 electrons. For UF_6, however, where these 5f occupations differ only by 0.20 electrons, the An–F bond energy is still reasonable, i.e. it deviates by 0.29 eV (5.1%). Thus, the 5f-in-core approximation seems to reach its limitations for the hexavalent oxidation state except for uranium, which corresponds to $5f^0$.

Figure 1, which shows the differences between LPP HF and SPP state-averaged MCSCF 5f occupations for actinide fluorides in different oxidation states AnF_n ($n = 2$–6) [8, 9], helps to clarify this conclusion. As one can see the 5f occupations for AnF_2, AnF_3, and AnF_4 differ at most by ca. 0.1 electrons except for ThF_3 ($Z = 90$) and PaF_3 ($Z = 91$). This explains the good performance of the 5f-in-core PPs for the di-, tri-, and tetravalent oxidation state. The reason for the large deviations in the case of Th and Pa is that for these actinides the trivalent oxidation state is not preferred

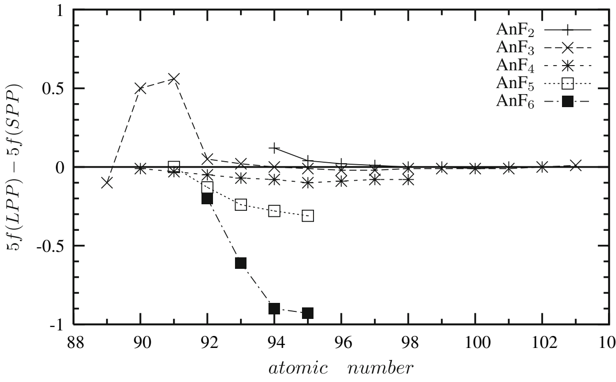

Fig. 1 Differences between LPP HF and SPP state-averaged MCSCF 5f orbital occupations for AnF_2 (An = Pu–No) [9], AnF_3 (An = Ac–Lr) [8], AnF_4 (An = Th–Cf) [9], AnF_5 (An = Pa–Am), and AnF_6 (An = U–Am). Basis sets: LPP (7s6p5d2f1g)/[6s5p4d2f1g]; SPP (14s13p10d8f6g)/[6s6p5d4f3g]; F aug-cc-pVQZ

(Th) or even not stable (Pa) in aqueous solution [44]. Thus, the trivalent subconfiguration $5f^n$ mixes strongly with the corresponding energetically low-lying tetravalent subconfiguration $5f^{n-1}6d^1$ yielding smaller SPP 5f occupations than assumed for the LPP core [8]. For AnF_5 the differences in the 5f occupations are slightly larger and differ by at most ca. 0.3 electrons. This difference is still acceptable, because the pentavalent PPs yield reasonable results for bond lengths and binding energies. For AnF_6, however, the deviations in the 5f occupations are significantly increased up to ca. 0.9 electrons, which explains the failure of the hexavalent PPs in the case of the AnF_6 binding energies. The larger deviations in the 5f occupations of AnF_5 and AnF_6 compared to those of AnF_2–AnF_4 are due to the fact that the higher the assumed oxidation state, the less probable it is, since ionization energies increase with increasing positive charge. Therefore, the reason for the failure of the hexavalent 5f-in-core PPs is that this formal oxidation state is not realized in the molecule, e.g. for AnF_6 the total atomic charges on the actinide amount at most to 4.10 instead of 6 units. For UF_6, however, one can see that the deviation in the 5f occupation is comparable to those of AnF_5, wherefore the hexavalent PP for uranium yields reasonable results. Finally, one can conclude that differences between LPP and SPP 5f occupations higher than 0.5 electrons become too big.

3.3 Uranyl ion

Table 4 Bond lengths *R* (in Å), ionic binding energies Δ*E* (in eV), and 5f orbital occupations for UO_2^{2+} from LPP HF, CCSD(T), and DFT calculations in comparison to corresponding SPP calculations as well as computational data from literature

Method	Ref.	*R*	Δ*E*	5f Occupation
LPP HF		1.631	176.05	1.74
SPP HF		1.639	181.21	2.23
AE DHF	[45]	1.650		
LPP CCSD(T)[a]		1.668	177.30	1.69
SPP CCSD(T)[a]		1.689	183.82	2.17
SPP CCSD[b]	[46]	1.697		
quasirel. AE CCSD(T)[b]	[47]	1.683		
AE DHF+CCSD(T)[b]	[48]	1.715		
LPP DFT/B3LYP		1.642	180.44	2.04
SPP DFT/B3LYP		1.692	185.85	2.45
SPP DFT/B3LYP	[47]	1.698		
quasirel. DFT/BPVWN[c]	[49]	1.716		

Basis sets: LPP (7s6p5d2f1g)/[6s5p4d2f1g]; SPP (14s13p10d8f6g)/[6s6p5d4f3g]; SPP DFT(14s13p10d8f6g)/[10s9p5d4f3g]; O aug-cc-pVQZ

[a] O 1s orbitals were kept frozen

[b] U 5s, 5p, and 5d as well as O 1s orbitals were kept frozen

[c] For U 1s–5d and O 1s orbitals the frozen-core approximation was applied

Table 4 shows bond lengths, ionic binding energies, and 5f orbital populations for UO_2^{2+} from LPP HF, CCSD(T), and DFT/B3LYP calculations in comparison to corresponding SPP calculations and computational data from literature [45–49]. As one can see the LPP and SPP U–O bond lengths are in good agreement, i.e. the LPP underestimates the SPP bond lengths by 0.008 (0.5%), 0.021 (1.3%), and 0.050 Å (3.0%) at the HF, CCSD(T), and DFT/B3LYP level, respectively. In comparison to the computational data from literature, the LPP bond lengths differ in a range of 0.015 (0.9%) to 0.074 Å (4.3%). However, these deviations are not necessarily due to the different core definitions, but may also result from the use of different basis sets, relativistic approaches, or density functionals. For example, in the case of the largest deviation, which occurs between the LPP DFT/B3LYP and the quasirelativistic DFT/BPVWN [49] calculation, a 1s–5d instead of a 1s–5f core, pTZ instead of aug-cc-pVQZ basis sets, and the BPVWNinstead of the B3LYP density functional were used for the quasirelativistic DFT calculation.

For the ionic binding energies the LPP underestimate the SPP data by 5.16 (2.8%), 6.52 (3.5%), and 5.41 eV (2.9%) for HF, CCSD(T), and DFT/B3LYP calculations, respectively. These small deviations as well as those for the U–O bond lengths can be understood by the comparison of the LPP and SPP 5f orbital occupations, which are for all calculations below 0.50 electrons, i.e. the differences between LPP and SPP 5f occupations are 0.49, 0.48, and 0.41 electrons for HF, CCSD(T), and DFT/B3LYP calculations, respectively. Thus, in contrast to the hexavalent LPPs for Np, Pu, and Am, the hexavalent LPP for uranium ($5f^0$) yields reasonable results.

3.4 Range of applications

The 5f-in-core PPs simplify electronic structure calculations on actinide compounds significantly. However, the assumption of a fixed near-integral 5f occupancy also bears the danger of misuse of the approach, e.g. for cases where another 5f occupancy than modeled by the PP is actually present, cases where states with different 5f occupancies mix, or systems where the 5f orbitals strongly contribute directly to chemical bonding in a MO-LCAO (molecular orbitals by linear combination of atomic orbitals) sense. Thus, we urge the users of the 5f-in-core PPs to verify the underlying assumption by (single-point) test calculations using, e.g. 5f-in-valence SPPs [6, 7] or AE methods at the HF level. It is clear that questions related to individual electronic states cannot be addressed with the present approach, which rather provides answers for an average over a multitude of states characterized by the same 5f occupancy and the same valence substate, i.e. a superconfiguration in the sense of the concept of Field advocated for lanthanides more than two decades ago [50].

The range of possible successful applications of the actinide 5f-in-core PPs is certainly somewhat smaller than for lanthanide 4f-in-core PPs [14], nevertheless, a quite significant part of actinide chemistry remains open for applications of the approach. However, in the case of the higher, namely the penta- and hexavalent, oxidation states the successful applications will noticeably decrease compared to those of the lower (di-, tri-, and tetravalent) oxidation states, because the higher oxidation states are only formally realized in molecules. But, for example, the investigation of UO_2^{2+} complexes using the hexavalent LPP should be feasible, since our test calculations for the bare uranyl ion yield reasonable results.

However, LPP HF test calculations [20] on AnO_2^+ (An = U–Am) and AnO_2^{2+} (An = Np–Am) actinyl ions assuming penta- and hexavalent actinides, respectively, do not yield linear structures as former scalar-relativistic AE DFT/PBE [51] and SPP restricted active space self-consistent field (RASSCF) [52] calculations, but bent structures with O–An–O bond angles between 102.2 and 109.3° (LPP HF: basis sets: An (7s6p5d2f1g)/[6s5p4d2f1g], O aug-cc-pVQZ [22, 23]; symmetry: C_{2v}). Furthermore, the LPP HF bond lengths are by about 0.029 (1.6%) and 0.112 Å (7.0%) longer than those of the AE DFT/PBE [51] and SPP RASSCF [52] reference data for AnO_2^+ and AnO_2^{2+}, respectively. Thus, in the case of these systems the a priori assumption of penta- and hexavalent actinides and a corresponding near-integral 5f occupancy seems to fail. We note that for UO_2^{2+} LPP HF geometry optimizations [34] using C_1 symmetry and different starting points always yield the correct linear structure, which was identified as a true energy minimum by a numerical vibrational frequency analysis.

In order to understand the discrepancies between the 5f-in-valence and 5f-in-core PP results, we performed a SPP state-averaged MCSCF geometry optimization [20] for UO_2^+ distributing one electron in the seven U 5f orbitals and optimizing the mean energy of the corresponding seven states (cf. Table 5; basis sets: U (14s13p10d8f6g)/[6s6p5d4f3g] [7], O aug-cc-pVQZ [22, 23]; symmetry: C_{2v}). Analogous to the LPP HF result the obtained SPP MCSCF structure is bent with a O–U–O bond angle of 152.1° ($R_e = 1.729$ Å). If the UO_2^+ structure is optimized for the individual states, four linear and three nonlinear structures are obtained (cf. Table 5). From a Mulliken population analysis of the singly occupied MOs (SOMOs), which are dominantly of U 5f character, it can be seen that the seven U 5f orbitals can be divided into two subgroups. Four of them are pure f orbitals (100% f character) and three have dominant f contributions, but mix with U d and O p orbitals (f character about 75–88%). The pure f orbitals are non-bonding f_δ and f_ϕ orbitals and when singly occupied the corresponding optimizations yield linear structures. The other f orbitals correspond for a linear structure to f_π and f_σ orbitals, which can mix with U d and O p orbitals due to their symmetry. If these orbitals are singly occupied the corresponding optimizations yield bent structures, which have a 2–3 eV higher energy than the linear ones with f_δ or f_ϕ singly occupied. The reason why in C_{2v} the optimization for the average of the seven states yields a bent structure, although there are more linear than nonlinear structures, is most likely that for the $^2B_2$ state the energy difference between the linear structure and the bent equilibrium structure is so high (3.63 eV) that the optimization of the mean energy $\bar{E}$ is dominated by this contribution and dragged to a bent structure. Since the

Table 5 U–O bond lengths R (in Å), bond angles ∠ O–U–O (in deg), and occupations of the SOMOs, which are dominantly of U 5f character, for UO_2^+ from SPP state-averaged MCSCF geometry optimizations for the energies of the individual states arising from a $5f^1$ occupation as well as for the mean energy of these states $\bar{E}$

Optimized for	R	∠	MO Occ.	ΔE	$\Delta E^{\mathrm{a}}_{\mathrm{linear}}$
$E(^2\Delta_u)$	1.700	180.0	1.00	0.00	
$E(^2\Phi_u)$	1.711	180.0	1.00	0.06	
$E(^2A_1)$	1.725	155.8	0.75	2.26	0.07
$E(^2B_1)$	1.736	117.8	0.88	2.03	0.30
$E(^2B_2)$	1.750	100.1	0.86	3.09	3.63
$\bar{E}$	1.729	152.1		1.66	0.14

Furthermore, the relative energies ΔE with respect to the lowest state $^2\Delta_u$ (in eV) and the energy difference $\Delta E_{\mathrm{linear}}$ (in eV) to a $D_{\infty h}$ optimized structure is given

Basis sets: U (14s13p10d8f6g)/[6s6p5d4f3g]; O aug-cc-pVQZ

[a] $\Delta E_{\mathrm{linear}} = E(D_{\infty h}) - E(C_{2v})$

pentavalent 5f-in-core PP for uranium describes the average of all $5f^1$ states, a bent UO_2^+ structure is obtained in qualitative agreement with the 5f-in-valence SPP result. However, it is obvious from the singly occupied orbital population analysis (cf. Table 5) that the assumption of a 5f occupancy of at least one electron is not fulfilled. Thus, UO_2^+ cannot be treated within the 5f-in-core approximation using the pentavalent PP for uranium.

However, if the hexavalent PP for uranium is applied to calculate UO_2^+ by explicitly distributing one electron in the seven f orbitals and optimizing the mean energy of the seven states, a similar structure as in the SPP MCSCF calculation with a bond angle of 160.5° ($R_e = 1.667$ Å) is obtained (basis sets: U (7s6p5d4f1g)/[6s5p4d4f1g], O aug-cc-pVQZ [22, 23]; symmetry: C_{2v}). Here, the uranium basis set has been slightly increased by using four instead of two f exponents, which have been optimized in state-averaged MCSCF calculations [20] for the $5f^3 6d^1 7s^2$ valence subconfiguration of the hexavalent LPP of uranium (exponents: 5.719, 2.062, 0.797, 0.266).

If HF instead of state-averaged MCSCF calculations are performed [20] by assuming the single electron to be, e.g. in a f_δ orbital, both SPP and LPP yield linear structures with a bond length difference of 0.058 Å (SPP: $R_e = 1.700$, LPP: $R_e = 1.642$ Å). Therefore, reasonable results are obtained for the UO_2^+ molecule with the LPP presented here, but the hexa- instead of the pentavalent PP for uranium has to be used. It should be noted, however, that the hexavalent PP for uranium is of large-core, but not really of 5f-in-core type ($5f^0$ occupation).

The other actinyl ions AnO_2^+ and AnO_2^{2+} (An = Np–Am) are similar to UO_2^+ and the failure of the penta- and hexavalent LPPs, respectively, should therefore also be due to the fact that states, where a f_π or f_σ orbital is occupied, yield nonlinear structures. In summary the application of the 5f-in-core approach to these systems cannot be recommended.

4 Conclusion

Quasirelativistic 5f-in-core PPs and corresponding valence basis sets have been generated for penta- and hexavalent actinide atoms. Atomic HF calculations using these PPs and uncontracted basis sets deviate at most by 0.15 eV from corresponding numerical PP HF results. The differences using the VQZ contraction of the (7s6p5d) basis sets stay below 0.03 and 0.06 eV for penta- and hexavalent PPs, respectively.

Results of HF and CCSD(T) test calculations on AnF_5 (An = Pa–Am) using 5f-in-core LPPs show reasonable agreement with corresponding SPP state-averaged MCSCF and AE/experimental data, respectively, i.e. the m.a.e. (m.r.e.) in bond lengths, angles, and energies amount at most to 0.037 Å (1.8%), 6.1° (6.1%), and 0.090 eV (1.7%), respectively. Thus, these 5f-in-core PPs should be reliable tools to investigate compounds including pentavalent actinides, whose 5f shell does not participate significantly in bonding.

In the case of the hexavalent PPs the results for the bond lengths of AnF_6 (An = U–Am) are satisfactory, i.e. LPP HF and LPP CCSD(T) bond lengths differ at most by 0.031 (1.6%) and 0.018 Å (0.9%) from SPP state-averaged MCSCF and experimental data, respectively. However, for binding energies the deviations between LPP and SPP results become as large as 0.80 eV (15.2%) indicating that in the hexavalent case the 5f-in-core approximation reaches its limitations and that therefore these PPs should only be used for preoptimizing purposes. This conclusion can also be drawn comparing the LPP and SPP 5f orbital occupations, which deviate by up to 0.93 electrons. Only for UF_6 this deviation is relatively small (0.20 electrons), wherefore here the LPP HF binding energy is still reasonable [0.29 eV (5.1%)]. Thus, the LPP for hexavalent uranium ($5f^0$) should yield reasonable results, which is also confirmed by the good agreement of LPP and SPP data in the case of UO_2^{2+} (maximum deviations: $\Delta R = 0.050$ Å (3.0%); $\Delta E = 6.52$ eV (3.5%); $\Delta 5f = 0.49$ electrons).

Finally, we want to emphasize again that the derived 5f-in-core PPs will only lead to reliable results for those cases where the An 5f occupation number is close to integral. We recommend to explicitly test this condition, e.g. in single-point HF calculations with an explicit treatment of the 5f shell, since it is not always obvious, where the limitations of the 5f-in-core approach are. For example in the case of the AnO_2^+ (An = U–Am) and AnO_2^{2+} (An = Np–Am) actinyl ions the assumption of a penta- and hexavalent An with fixed near-integral 5f occupation is invalid yielding bent instead of linear molecular structures, although for UO_2^{2+} the results are reasonable.

Acknowledgments The financial support from the Deutsche Forschungsgemeinschaft (DFG) to A.M. is gratefully acknowledged.

References

1. Katz JJ, Seaborg GT, Morss LR (1986) The chemistry of the actinide elements, vol 2. Chapman and Hall, London
2. Pepper M, Bursten B (1991) Chem Rev 91:719
3. Schreckenbach G, Hay PJ, Martin RL (1999) J Comput Chem 20:70
4. Dolg M, Cao X (2003) The relativistic energy-consistent ab initio pseudopotential approach. In: Hirao K, Ishikawa Y (eds) Recent advances in relativistic molecular theory. World Scientific, New Jersey
5. Cao X, Dolg M (2006) Coord Chem Rev 250:900

6. Küchle W, Dolg M, Stoll H, Preuss H (1994) J Chem Phys 100:7535
7. Cao X, Dolg M, Stoll H (2003) J Chem Phys 118:487
8. Moritz A, Cao X, Dolg M (2007) Theor Chem Acc 117:473
9. Moritz A, Cao X, Dolg M (2007) Theor Chem Acc 118:845
10. Cao X, Li Q, Moritz A, Xie Z, Dolg M, Chen X, Fang W (2006) Inorg Chem 45:3444
11. Wiebke J, Moritz A, Cao X, Dolg M (2007) Phys Chem Chem Phys 9:459
12. Moritz A, Dolg M (2007) Chem Phys 337:48
13. Evarestov RA, Losev MV, Panin AI, Mosyagin NS, Titov AV (2008) Phys Stat Sol (b) 245:114
14. Dolg M, Stoll H, Savin A, Preuss H (1989) Theor Chim Acta 75:173
15. Dolg M, Stoll H, Preuss H (1989) J Chem Phys 90:1730
16. Küchle W, Dolg M, Stoll H, Preuss H (1991) Mol Phys 74:1245
17. Froese Fischer C (1977) The Hartree–Fock method for atoms. Wiley, New York; program MCHF77, modified for pseudopotentials and quasirelativistic calculations by Dolg M (1995)
18. Dolg M, Stoll H, Preuss H (1993) Theor Chim Acta 85:441
19. Pitzer RM (1979) Atomic electronic structure code ATMSCF. The Ohio State University, Columbus
20. Amos RD, Bernhardsson A, Berning A, Celani P, Cooper DL, Deegan MJO, Dobbyn AJ, Eckert F, Hampel C, Hetzer G, Knowles PJ, Korona T, Lindh R, Lloyd AW, McNicholas SJ, Manby FR, Meyer W, Mura ME, Nicklass A, Palmieri P, Pitzer R, Rauhut G, Schütz M, Schuhmann U, Stoll H, Tarroni AJSR, Thorsteinsson T, Werner HJ (2002) MOLPRO is a package of ab initio programs. University of Birmingham
21. http://www.theochem.uni-stuttgart.de/pseudopotentials
22. Dunning Jr TH (1989) J Chem Phys 90:1007
23. Kendall RA, Dunning Jr TH, Harrison RJ (1992) J Chem Phys 96:6796
24. Kovacs A, Konings RJM, Nemcsok DS (2003) J Alloys Compd 353:128
25. Jones LH, Ekberg S (1977) J Chem Phys 67:2591
26. Kimura M, Schomaker V, Smith DW (1968) J Chem Phys 48:4001
27. Seip HM (1965) Acta Chem Scand 19:1955
28. Becke AD (1993) J Chem Phys 98:5648
29. Lee C, Yang W, Parr RG (1988) Phys Rev B 37:785
30. Becke AD (1988) Phys Rev A 38:3098
31. Vosko SH, Wilk L, Nusair M (1980) Can J Phys 58:1200
32. Slater JC (1951) Phys Rev 81:385
33. Dirac PAM (1930) Proc Cambr Phil Soc 26:376
34. Ahlrichs R, Bär M, Baron HP, Bauernschmitt R, Böcker S, Ehrig M, Eichkorn K, Elliott S, Furche F, Haase F, Häser M, Horn H, Huber C, Huniar U, Kölmel C, Kollwitz M, Ochsenfeld C, Öhm H, Schäfer A, Schneider U, Treutler O, Arnim M, Weigend F, Weis P, Weiss H (2004) TURBOMOLE v. 5.7 University of Karlsruhe
35. Cao X, Dolg M (2004) J Mol Struct 673:203
36. Dolg M, Stoll H (1989) Theor Chim Acta 75:369
37. Dyall KG, Grant IP, Johnson CT, Parpia FA, Plummer EP (1989) GRASP: atomic structure code. Comput Phys Commun 55:425
38. http://www.lac.u-psud.fr/Database/Contents.html
39. Wadt WR, Hay PJ (1979) J Am Chem Soc 101:5198
40. Batista ER, Martin RL, Hay PJ (2004) J Chem Phys 121:11104
41. Hay PJ, Martin RL (1998) J Chem Phys 109:3875
42. Han YK (2001) J Comput Chem 22:2010
43. Batista ER, Martin RL, Hay PJ, Peralta JE, Scuseria GE (2004) J Chem Phys 121:2144
45. Kaltsoyannis N, Scott P (1999) The f elements. Oxford University Press, Oxford
45. Dyall KG (1999) Mol Phys 96:511
46. Cornehl HH, Heinemann C, Marcalo J, Pires de Matos A, Schwarz H (1996) Angew Chem, Int Edn 35:891
47. Real F, Vallet V, Marian C, Wahlgren U (2007) J Chem Phys 127:214302
48. de Jong WA, Visscher L, Nieuwpoort WC (1999) J Mol Struct 458:41
49. Kaltsoyannis N (2000) Inorg Chem 39:6009
50. Field RW (1982) Ber Bunsenges Phys Chem 86:771
51. Shamov GA, Schreckenbach G, Martin RL, Hay PJ (2008) Inorg Chem 47:1465
52. Vallet V, Maron L, Schimmelpfennig B, Leininger T, Teichteil C, Gropen O, Grenthe I, Wahlgren U (1999) J Phys Chem A 103:9285